*Int. J. Electrochem. Sci.*, 13 **(2018)** 11263 – 11272, doi: 10.20964/2018.11.72

International Journal of
ELECTROCHEMICAL
SCIENCE
www.electrochemsci.org

# Electrochemical and Theoretical Study of Imidazole Derivative as Effective Corrosion Inhibitor for Aluminium

*Jinchang Wang[1,3], Ambrish Singh[1,2,*], Mohd Talha[1,2,], Xi Luo[3], Xuefeng Deng[3],Yuanhua Lin[1,2,4*]*

[1] School of Materials Science and Engineering, Southwest Petroleum University, Chengdu-610500, Sichuan, China.
[2] State Key Laboratory of Oil and Gas Reservoir Geology and Exploitation, Southwest Petroleum University, Chengdu, Sichuan 610500, China
[3] North China Oil and Gas Branch Company of SINOPEC, Zhengzhou, Henan 450006, China
[4] CNPC Key Lab for Tubular Goods Engineering (Southwest Petroleum University), Chengdu, Sichuan 610500, China
[*]E-mail: yhlin28@163.com; vishisingh4uall@gmail.com

*Received:* 8 February 2018 / *Accepted:* 28 March 2018 / *Published:* 1 October 2018

The corrosion inhibition performance of 2-styryl-1,8-dihydro-1,3,8-triaza-cyclopentaindene (IIZ) on Aluminium in 1M HCl was investigated by electrochemical impedance spectroscopy (EIS), Potentiodynamic polarization, scanning electron microscopy (SEM), atomic force microscopy (AFM), and quantum chemical techniques. Potentiodynamic polarization study confirmed that IIZ is mixed type inhibitor with cathodic predominance. SEM and AFM confirm the formation of an adsorption film on the aluminium surface. Quantum chemical study reveals that protonated IIZ interacts more than neutral IIZ. The theoretical data obtained are in agreement with experimental results.

**Keywords:** Aluminium; Imidazole derivative, Corrosion; Electrochemical; AFM

## 1. INTRODUCTION

Corrosion of aluminium and its alloys has been a subject of numerous studies due to their high technological value and wide range of industrial applications especially in aerospace and household industries. Aluminium and its alloys are reactive materials and are prone to corrode [1]. Aluminium relies on the formation of a compact, adherent passive oxide film for its corrosion immunity in various environments. This surface film is amphoteric and dissolves substantially when the metal is exposed to high concentrations of acids and bases [2, 3]. Aluminium has wide application in day to day life such as reaction vessels, pipes, machinery and chemical batteries.

HCl is usually used in industry for acid cleaning, chemical or electrochemical etching and acid pickling of aluminium, but at same time it causes its corrosion. The solubility of oxide film increases

above and below pH 4-9 range and aluminium gets prone to uniform attack. Therefore, in order to isolate aluminium from HCl corrosion inhibitors are used [4-9]. These inhibitor molecules show their inhibiting property by being adsorbed on the aluminium surface, either physically or chemically or both through N, O, S and P as well as conjugate double bonds or π- electrons in aromatic ring.

In literature different derivatives of imidazole were used as corrosion inhibitors on different metals [10-12]. Despite the large number of imidazole derivative have been used as corrosion inhibitors, but less information is available regarding effective corrosion inhibitors for aluminium in HCl solution [13]. So, there is always a need for developing new and more effective corrosion inhibitors for aluminium and its alloys. In the recent years quantum chemical calculations has been extensively used for correlating the molecular structure of inhibitors and their inhibition properties [14]

The aim of this study is to investigate the inhibition effect of 2-styryl-1,8-dihydro-1,3,8-triaza-cyclopentaindene (IIZ) on the corrosion of aluminium in 1M HCl solution using electrochemical techniques (electrochemical impedance spectroscopy and potentiodynamic polarization), SEM, AFM and quantum chemical calculation.

## 2. EXPERIMENTAL

### *2.1. Materials*

1M HCl (test solution) was prepared by diluting 37% analytical grade HCl with double distilled water. Composition of aluminum sample used is as follows (wt.%): Si = 0.77, Fe=0.93, Cu=0.02, Mn=0.11, Mg=0.01, Zn=0.01, Cr=0.05, Ti=0.02, V=0.01, Ga=0.01 and balance Al. Aluminium strips with an exposed area of 1 $cm^2$ were used for electrochemical experiments.

### *2.2. Inhibitor*

The investigated organic compounds were synthesized according to the previously reported procedure [15]. Their chemical structure and abbreviation are given in Fig. 1.

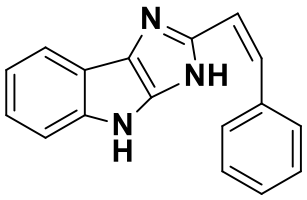


**Figure 1**. Chemical structure of 2-styryl-1,8-dihydro-1,3,8-triaza-cyclopentaindene (IIZ).

### *2.3. Electrochemical measurements*

Gamry Potentiostat /Galvanostat (Model G-300) was used for all electrochemical tests and data analyses were performed using Echem Analyst 5.0. A traditional cell where aluminium strip was used as working electrode, platinum as counter and saturated calomel as reference electrodes were used for the

tests. EIS measurements were carried out using frequency range of 100 kHz to 0.01 Hz at open circuit potential (OCP). The polarization tests were performed at -250 to +250 mV versus SCE. The scan rate was kept 1 $mVs^{-1}$ to get a clear and uninterrupted anodic and cathodic curve.

All the impedance and polarization tests were done at room temperature. Immersion time of 30 minutes was used to get a stable potential prior to the start of each electrochemical tests.

### *2.4. Surface morphology*

The surface of the aluminium samples were scanned with Ziess SUPRA 40 and NT-MDT SOLVER Next AFM/STM instruments to get SEM and AFM images. Prior to the tests the aluminium samples were immersed in 1M HCl with and without IIZ for 3 hours at room temperature. Gold (Au) spray was used on the aluminium samples to get better pictures of the surface through SEM.

### *2.5. Quantum chemical study*

The IIZ molecule was optimized using Gaussian-09 software equipped with Density Functional Theory (DFT) function through B3LYP module [16]. The optimization of the molecule was done in aqueous phase. The inhibitor molecule was studied in neutral and protonated form to explore new findings and orientations. Several relative quantum parameters including energy of the highest occupied molecular orbital ($E_{HOMO}$), energy of the lowest unoccupied molecular orbital ($E_{LUMO}$) and Energy gap ($\Delta E$) were obtained and discussed to support the experimental results.

## 3. RESULTS AND DISCUSSION

### *3.1. Electrochemical measurements*

#### *3.1.1. Electrochemical impedance spectroscopy*

Fig. 2 shows Nyquist plots in absence and presence of IIZ at different concentration at 308 K.

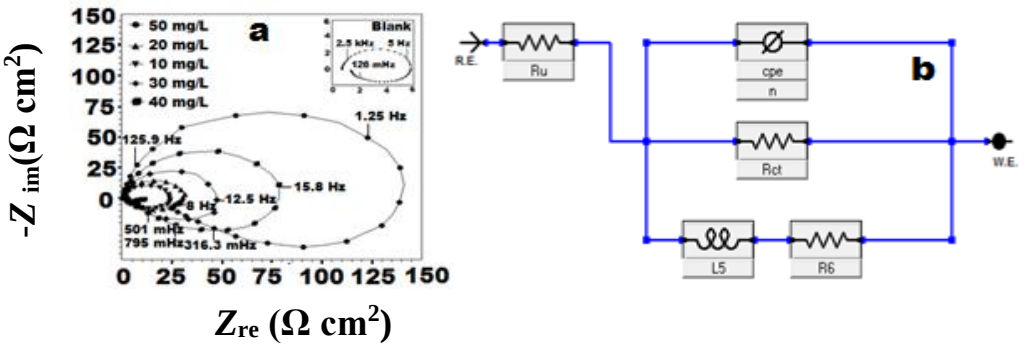


**Figure 2**. (a) Nyquist plots for aluminium in absence and presence of different of IIZ, (b) equivalent circuit

**Table 1**. EIS parameters for the corrosion of aluminium in 1M HCl solution containing different concentrations of IIZ at 308 K (immersion time 3h)

| Inhibitor | Conc. mg/L | $R_s$ ($\Omega$ cm$^2$) | $R_t$ ($\Omega$ cm$^2$) | $R_L$ ($\Omega$ cm$^2$) | $L$ (H cm$^2$) | $R_P$ ($\Omega$ cm$^2$) | $CPE$ ($\mu$F cm$^{-2}$) | ($\eta$%) | $X^2$ |
|---|---|---|---|---|---|---|---|---|---|
| Blank | - | 0.757 | 5.1 | 0.8 | 0.756 | 0.691 | 157.7 | - | $0.78\times10^{-2}$ |
| IIZ | 10 | 0.658 | 24.12 | 1.797 | 2.024 | 1.67 | 46.4 | 58.6 | $17.7\times10^{-2}$ |
| | 20 | 0.709 | 29.83 | 2.118 | 3.047 | 1.97 | 25.5 | 64.9 | $1.3\times10^{-2}$ |
| | 30 | 0.606 | 46.50 | 2.351 | 2.985 | 2.23 | 52.2 | 69.0 | $1.3\times10^{-2}$ |
| | 40 | 0.716 | 81.46 | 7.566 | 3.341 | 6.92 | 51.0 | 90.0 | $5.4\times10^{-2}$ |
| | 50 | 0.598 | 142.2 | 34.57 | 27.71 | 27.80 | 53.4 | 97.5 | $0.87\times10^{-2}$ |

The Nyquist plot reveals the presence of large capacitive loop at higher frequencies (HF) and a large inductive loop at low frequency (LF). In literature, it is said that [17], aluminium corrosion in HCl consist of a small inductive loop at LF as compared to capacitive loop. But, in the present study it consists of inductive loop which is almost equal in size to that of the capacitive loop [18].

In order to find the electrochemical parameters an equivalent circuit was used and is shown in Fig.2 (b). The components of this circuit consist of $R_s$ (solution resistance), $R_t$ (charge transfer resistance), *CPE* (constant phase element), $R_L$ (inductive resistance) and $L$ (inductance) respectively. The polarization resistance ($R_p$) and inhibition efficiency ($\eta$%) were calculated from the following equation [19]:

$$R_P = \frac{R_t R_L}{R_t + R_L} \quad (1)$$

$$\eta\% = \frac{R_{P(inh)} - R_{P(0)}}{R_{P(inh)}} \quad (2)$$

where $R_{p(0)}$ and $R_{p(inh)}$ are polarization resistance in the absence and presence of inhibitor, respectively. The impedance parameters are listed in Table 1. The precision of the fitted data was evaluated by chi-squared ($\chi^2$) [20]. The values of $\chi^2$ are very small (Table 1), which supports that the equivalent circuit is ideal for fitting. Also, the values of $R_s$ are very small, which confirms that the IR drop is small in the present experiments. The values of both $R_t$ and $R_p$ increases as the IIZ inhibitor is added, revealing the slow corrosion rate in presence of IIZ. Also, the *CPE* values are smaller in presence of IIZ then in its absence, which is due to decrease in local dielectric constant and/or an increase in the thickness of the electrical double layer, suggesting the adsorptive nature of IIZ inhibitor [21].

### *3.1.2. Potentiodynamic polarization*

The changes in the anodic and cathodic polarization curves at 308 K in 1M HCl were obtained and are given in Fig.3.

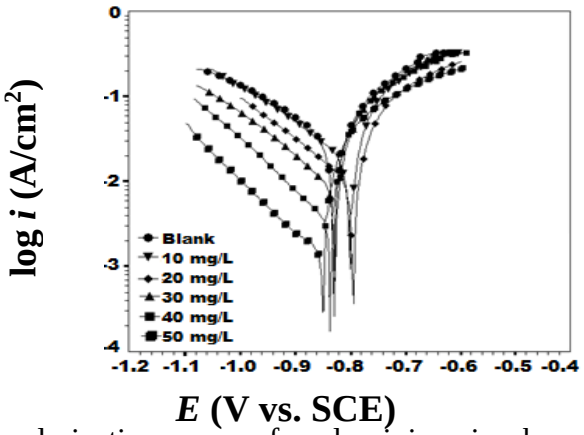


**Figure 3**. Potentiodynamic polarization curves for aluminium in absence and presence of different concentration of IIZ at 308 K

**Table 2.** Potentiodynamic polarization parameters for the corrosion of aluminium in 1M HCl solution containing different concentrations of IIZ at 308 K (immersion time 3h)

| **Inhibitor** | **Conc. mg/L** | $E_{corr}$ **(mV/SCE)** | $i_{corr}$ **(μA/cm$^2$)** | $-\beta_c$ **(mV/dec)** | **η (%)** |
|---|---|---|---|---|---|
| **Blank** | -- | -828.6 | 29790 | 247.9 | -- |
| **IIZ** | 10 | -801.4 | 13140 | 234.0 | 55.89 |
| | 20 | -798.5 | 9978 | 200.0 | 66.50 |
| | 30 | -826.6 | 8989 | 197.2 | 69.82 |
| | 40 | -835.9 | 3191 | 159.0 | 89.28 |
| | 50 | -849.4 | 1187 | 157.8 | 96.01 |

Both cathodic and anodic curves shift towards lower current density and the $E_{corr}$ value shows no definite trend. The $E_{corr}$ values drift both towards cathodic and anodic side which suggests that IIZ is acting as mixed type inhibitor. Here anodic regions are not linear subsequently; the corrosion current density ($i_{corr}$) values are obtained by exploring the linear region of only cathodic curves up to the corrosion potential [22].

The electrochemical parameters including corrosion potential ($E_{corr}$), corrosion current density ($i_{corr}$), inhibition efficiency ($\eta$%) and cathodic slope ($\beta_c$) are given in Table 2. The $\eta$% values are calculated by using the following equation [23].

$$\eta\% = \left(1 - \frac{I_{corr(i)}}{I_{corr}}\right) \times 100 \qquad (3)$$

It can be easily revealed from Table 2 that $i_{corr}$ values in the presence of IIZ are lower than in its absence [24-26]. There is significant change in cathodic slope ($\beta_c$) values at different concentration of IIZ, which corresponds towards the dominant cathodic side. So, to conclude it could be said that the inhibition action of IIZ is mixed type but favoring more cathodic inhibition [27-29].

*3.2 Surface morphology*

SEM-EDX images of the aluminium metal samples are shown in Fig. 4 (a-b).

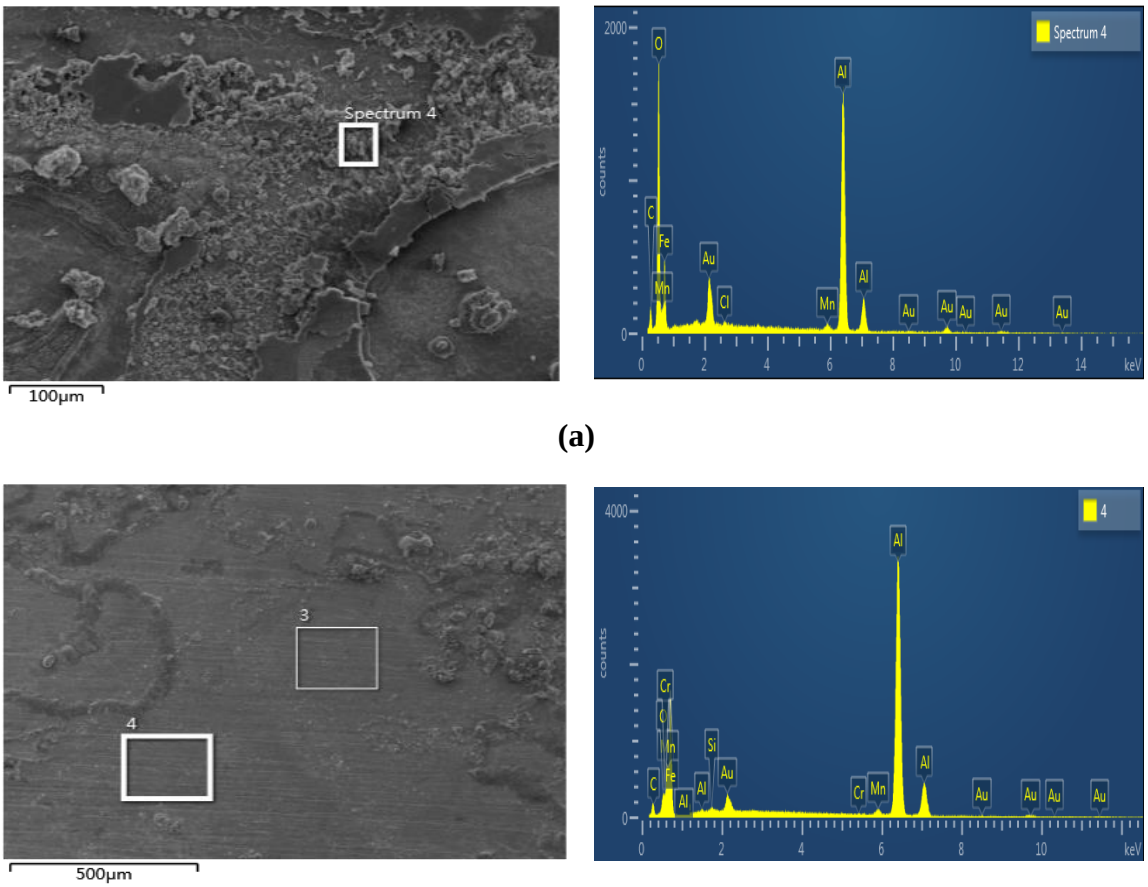


**Figure 4 a-b:** SEM-EDX images of (a) Aluminium metal after immersion in 1 M HCl for 3h (b) Aluminium metal after immersion in 1M HCl + IIZ for 3h.

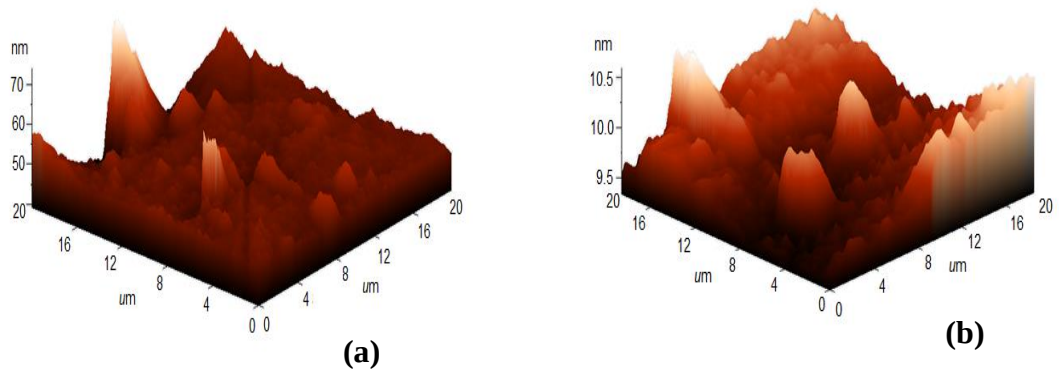


**Figure 5**. AFM images (a) unhibited surface (b) Surface inhibited with IIZ inhibitor.

Aluminium surface in absence of inhibitors is severely damaged (Fig 4 a), whereas, in the presence of IIZ (Fig. 4b), the corrosion was suppressed. The deposits of corrosion products may be seen

on the surface but the surface is uniform and smooth. This smooth surface reveals the adsorption of IIZ on aluminium surface.

The three dimensional (3D) AFM morphologies in absence and presence of inhibitors are given in Fig 5 (a-b).

Fig. 5a represents the morphology in absence of IIZ, which have higher peak height corresponding to severe corrosion. Fig.5b corresponds to the morphology in presence of IIZ and its peak height is lower as compared in its absence. This variation in peak height reveals that IIZ molecules have been adsorbed over the aluminium surface and checked the corrosion process.

### *3.3. Quantum Chemical Calculation*

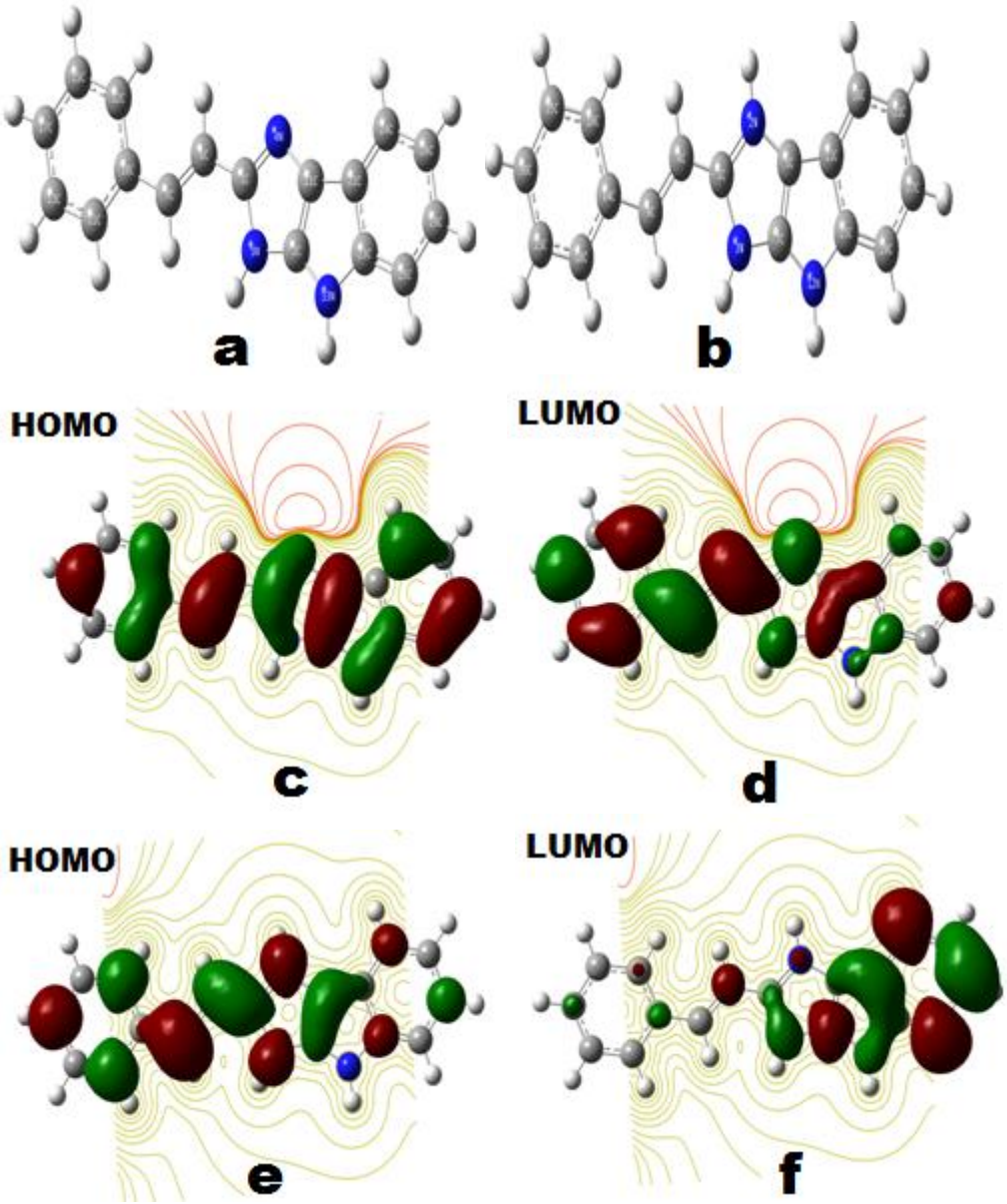


**Figure 6**: (a) optimized geometry of neutral IIZ (b) optimized geometry of protonated IIZ (c) neutral IIZ HOMO (d) neutral IIZ LUMO (e) protonated IIZ HOMO (f) protonated IIZ LUMO

The optimized geometry, HOMO, and LUMO orbital's for both neutral and protonated IIZ molecule in aqueous phase are shown in Fig. 6 (a-f).

It could be seen that HOMO and LUMO orbital's of neutral species and HOMO of protonated species are spread on the entire molecule, which suggests a flat or parallel adsorption of the IIZ molecules on the aluminium surface. This would provide a strong adsorption on the aluminium surface and thereby gives high inhibition efficiency. The electronic parameters related to the reactivity of the IIZ are reported in Table 3.

**Table 3.** Quantum chemical parameters of neutral and protonated IIZ

| **Quantum chemical parameters** | **IIZ** | **IIZ-p** |
|---|---|---|
| $E_{HOMO}$ **(eV)** | -4.918 | -2.948 |
| $E_{LUMO}$ **(eV)** | -1.363 | -0.207 |
| $\Delta E$ **(eV)** | 3.555 | 2.740 |

The electron donating tendency is represented by $E_{HOMO}$ values. Higher the value of $E_{HOMO}$ greater is its electron donating tendency. It can be observed from Table 3, that the electron-donating tendency is greater in protonated species (IIZ-p) than neutral species because of the greater values of $E_{HOMO}$ of protonated species.

The electron accepting capacity of a molecule is given by $E_{LUMO}$ values. The lower $E_{LUMO}$ is, the greater is the ability of that molecule to accept electrons. As can be seen in Table 3, that neutral species has lower value of $E_{LUMO}$ value as compared to protonated species and thus has greater electron accepting capacity.

But the most important parameter is $\Delta E$, which is the energy difference between LUMO and HOMO. The lower value of $\Delta E$ will facilitate the release of electron and stronger would be the adsorption. $\Delta E$ value of IIZ-p is lower than IIZ, which causes IIZ-p to easy electron release and in turn strengthen its adsorption. Also, $\Delta E$ values suggest that IIZ-p has more reaction capacity than neutral one. So, over all in the aqueous media IIZ-p has more interaction ability than neutral one towards aluminium surface.

## 4. CONCLUSION

1. EIS measurement showed two loops one at higher frequency and other at lower frequency but both are of similar size.
2. Potentiodynamic polarization reveals that IIZ is mixed type inhibitor but favoring more cathodic reaction suppression.
3. Both SEM and AFM show the adsorption of IIZ molecules.
4. Quantum chemical study reveals that protonated IIZ interacts more than neutral IIZ.

ACKNOWLEDGEMENTS
Authors are thankful to the Sichuan 1000 Talent Fund and financial assistance provided by the National Natural Science Foundation of China (No. 51274170).

**References**

1. I. B. Obot, N.O. Obi-Egbedi, S.A. Umoren, *Corros. Sci.*, 51 (2009) 1868.
2. Ambrish Singh, Ishtiaque Ahamad, Mumtaz A. Quraishi, *Arab. J. Chem*., 9 (2016) s1584.
3. Klodian Xhanari, Matjaž Finšgar, *Arab. J. Chem*., (2016) http://dx.doi.org/10.1016/j.arabjc.2016.08.009.
4. Shuduan Deng, Xianghong Li, *Corros. Sci.*, 64 (2012) 253.
5. Kazem Sabet Bokati, Changiz Dehghanian, *J. Environ. Chem. Eng*., 6 (2018) 1613.
6. Mahmoud N. El-Haddad, A.S. Fouda, *J. Mol. Liq*., 209 (2015) 480.
7. Z. Cao, Y. Tang, H. Cang, J. Xu, G. Lu, W. Jing, *Corros. Sci*., 83 (2014) 292.
8. K. Zhang, B. Xu, W. Yang, X. Yin, Y. Liu, Y. Chen, *Corros. Sci*., 90 (2015) 284.
9. J. Aljourani, K. Raeissi, M.A. Golozar, *Corros. Sci*., 51 (2009) 1836.
10. K. F. Khaled, Mohammed A. Amin, *J. Appl. Electrochem*., 39 (2009) 255.
11. K.R. Ansari, M.A. Quraishi, A. Singh, *Measurement*, 76 (2015) 136.
12. N. Kumar, P.K. Sharma, V. K. Garg, P. Singh, *Curr. Res. Chem*., 3 (2011)114.
13. Gaussian 03, Revision E.01, M. J. Frisch, G.W. Trucks, H. B. Schlegel, G. E. Scuseria, M. A. Robb, J. R. Cheeseman, Jr. J. A. Montgomery, T. Vreven, K. N. Kudin, J. C. Burant, J. M. Millam, S. S. Iyengar, J. Tomasi, V. Barone, B. Mennucci, M. Cossi, G. Scalmani, N. Rega, G. A. Petersson, H. Nakatsuji, M. Hada, M. Ehara, K. Toyota, R. Fukuda, J. Hasegawa, M. Ishida, T. Nakajima, Y. Honda, O. Kitao, H. Nakai, M. Klene, X. Li, J. E. Knox, H. P. Hratchian, J. B. Cross, V. Bakken, C. Adamo, J. Jaramillo, R. Gomperts, R. E. Stratman, O. Yazyev, A. J. Austin, R. Cammi, C. Pomelli, J. W. Ochterski, P. Y. Ayala, K. Morokuma, G. A. Voth, P. Salvador, J. J. Dannenberg, V. G. Zakrzewski, S. Dapprich, A. D. Daniels, M. C. Strain, O. Farkas, D.K. Malick, A.D. Rabuck, K. Raghavachari, J.B. Foresman, J.V. Ortiz,Q. Cui, A.G. Baboul, S. Clifford, J. Cioslowski, B.B. Stefanov, G. Liu, Liashenko, A .P. Piskorz, I. Komaromi, R. L. Martin, D. J. Fox, T. Keith, M. A. Al-Laham, C. Y. Peng, A. Nanayakkara, M. Challacombe, P. M. W. Gill, B. Johnson, W. Chen, M. W. Wong, C. Gonzalez, J. A. Pople, Gaussian, Inc., Wallingford CT, (2007).
14. K.F. Khaled, M. M. A. Qahtani, *Mater. Chem. Phys*., 113 (2009) 150.
15. S. Parveen, T. Ahamad, A. Malik, N. Nishat, *Polym. Adv. Technol*., 19 (2008) 1779.
16. W. R. Osório, D. J. Moutinho, L. C. Peixoto, I. L. Ferreira, A. Garcia, *Electrochim Acta*., 56 (2011) 8412.
17. W. J. Lorenz, F. Mansfeld, *Corros Sci*., 21 (1981) 647.
18. X. H. Li, S. D. Deng, H. Fu, *Corros Sci*., 53 (2011) 1529.
19. A. Singh, K. R. Ansari, X. Xu, Z. Sun, A. Kumar, Y. Lin, *Sci. rep*., 7 (2017) 14904.
20. A. Singh, K. R. Ansari, A. Kumar, W. Liu, C. Songsong, Y. Lin, *J. Alloys Comp.*, 76 (2017) 61.
21. Ambrish Singh, Yuanhua Lin, I. B. Obot, E. E. Ebenso, K. R. Ansari, M. A. Quraishi, *Appl. Surf. Sci*., 356 (2015) 341.
22. K. R. Ansari, M. A. Quraishi, A. Singh, *Corros Sci*., 79 (2014) 5.
23. A. Singh, K. R. Ansari, J. Haque, P. Dohare, H. Lgaz, R. Salghi, M. A. Quraishi, *J. Taiwan Inst. Chem. Eng.*, 82 (2018) 233.
24. K. R. Ansari, M. A. Quraishi, *Anal. Bioanal. Electrochem*., 7( 2015) 509.
25. D. G. Ladha, P. M. Wadhwani, M. Y. Lone, P. C. Jha, and N. K. Shah, *Anal. Bioanal. Electrochem*., 7 (2015) 59.

26. A. Fattah-alhosseini, A. Moradi, E. Moradi, and N. Attarzadeh, *Anal. Bioanal. Electrochem*., 6 (2014) 284.
27. A. Singh, Yuanhua Lin, Wanying Liu, Deng Kuanhai, Jie Pan, Bo Huang, Chengqiang Ren, D. Zeng, *J. Taiwan Inst. Chem. Engg*., 45 (2015) 1918.
28. Ambrish Singh, Yuanhua Lin, E. E. Ebenso, Wanying Liu, Jie Pan, B. Huang, *J. Ind. Engg. Chem*., 24 (2015) 219.
29. K. R. Ansari, M. A. Quraishi, A. Singh, *Corros. Sci.*, 95 (2015) 62.